



Molecular Dynamics, Smoothed-Particle Applied Mechanics, and Irreversibility

W. G. HOOVER, T. G. PIERCE, C. G. HOOVER
J. O. SHUGART, C. M. STEIN, AND A. L. EDWARDS
Department of Applied Science
University of California at Davis/Livermore
and
Lawrence Livermore National Laboratory
Livermore, CA, 94551-7808, U.S.A.

Abstract—We explore the relationship of Monaghan's version of "smoothed-particle hydrodynamics," here called "smoothed-particle applied mechanics," to nonequilibrium molecular dynamics. We first use smoothed particles to model the simplest possible linear transport problems, as well as a liquid-drop problem. We then consider both gas-phase and dense-fluid versions of Rayleigh-Bénard convection, all in two space dimensions. We also discuss the possibility of combining the microscopic and macroscopic techniques in a hybrid scheme well-suited to the massively-parallel modelling of large-scale nonequilibrium flows.

1. INTRODUCTION

There are two distinct approaches (see, for example [1,2]; see then [3-5]) to the numerical simulation of nonequilibrium flows, microscopic "molecular dynamics" and macroscopic "continuum mechanics." Both are based on the solution of sets of deterministic differential equations. The microscopic approach is based on the solution of *time-reversible* ordinary differential equations for the motion of atoms. At equilibrium, the motion is governed by Newtonian coordinate-dependent forces, $\{F(r)\}$. Newtonian mechanics can be extended, to treat nonequilibrium problems, still maintaining time reversibility, by including deterministic momentum-dependent external forces to control velocities, energies, temperatures, stresses, and heat fluxes. A "solution" of the microscopic problem gives the time-dependence of all the atomic coordinates $\{r(t)\}$. The microscopic motion is typically "chaotic," that is, exponentially sensitive to small perturbations.

The *macroscopic* approach to simulation is based on the solution of the partial differential field equations for the space-and-time evolution of the continuum field variables: mass density, velocity, and energy density $\{\rho(r, t), v(r, t), e(r, t)\}$. Here, the *time-irreversible* motion is governed by the constitutive relations expressing the pressure tensor P and heat flux vector Q in terms of the field variables and their gradients. Often, with stationary boundary conditions, the continuum solutions are stationary or periodic in time. Though the continuum description only applies, in principle, to an infinite number of degrees of freedom, the conventional approach ignores, as

This work was performed, in part, under the auspices of the United States Department of Energy at the Lawrence Livermore National Laboratory, supported by Contract W-7405-Eng-48. M. Gibbons, and especially L. Cloutman and O. Kum, provided useful suggestions and advice. We have also benefitted from conversations with H. Posch and O. Richmond. L. Brookshaw's treatment of the surface radiation from stars suggested our own treatment of liquid-drop surface tension. He has also studied a variety of smoothed-particle representations of the continuum equations for heat conduction. Brookshaw's work was recently summarized in the proceedings of the OAT-SISSA International Workshop on Smoothed Particle Hydrodynamics in Astrophysics (Trieste, July, 1993).

unnecessary and irrelevant, the high-frequency short-wavelength chaotic *fluctuations* present in microscopic molecular dynamics. But the remaining long-wavelength continuum motion can also be chaotic, as is evidenced by turbulent flows.

Problems described by the partial differential equations of continuum mechanics are usually solved with grid-based Eulerian or Lagrangian computer-simulation programs. Much less effort has been applied to the development of grid-free methods. By avoiding the logical complexity of dealing with the tangling and geometric instabilities associated with large deformation, these grid-free methods provide a relatively simple approach to the simulation of complex flows in two or three space dimensions. We will see that one of these grid-free methods, usually termed “Smoothed-Particle Hydrodynamics,” is closely related to conventional molecular dynamics. Because the method is applicable to solids, as well as to fluids other than water, we have adopted the name “Smoothed-Particle Applied Mechanics” for this macroscopic approach.

With either the microscopic or the macroscopic approach, a “large-sized” numerical simulation today (1994) involves millions (or even billions!) of degrees of freedom. But a cubic micron of metal contains about a *hundred billion* atoms. In fracture, tribology, and materials science there is thus an urgent need for particle-based continuum methods to help bridge the wide gap between the atomistic and continuum length scales. A variety of nonequilibrium problems on the micron to nanometer scale require a treatment of atomic degrees of freedom for accuracy, but are much too large and too slow for a comprehensive treatment with the atomistic approach.

We will see that a hybrid scheme, in which an atomic description of the most active part of the flow is embedded in a simpler surrounding continuum, can be based on a combination of the microscopic and macroscopic techniques. Both the microscopic and the macroscopic simulation schemes, as well as this developing hybrid combination, incorporate only local short-ranged interactions. Thus, these schemes are all well-matched to today’s massively-parallel computers [6].

In the present work, we first consider an interesting formal connection between molecular dynamics and smoothed-particle mechanics. Next, we apply the smoothed-particle approach to the simulation of two simple linear nonequilibrium fluid flows, using simple ideal-gas mechanical and thermal equations of state. The first of these test problems is Fourier heat conduction, between two fixed walls maintained at different temperatures. The second nearly-linear test problem is plane Couette flow, in which two thermostatted shearing walls move in opposite directions, imposing a velocity gradient. We then discuss two smoothed-particle methods for treating free surfaces, and surface tension, and apply the simpler of these choices to the structure of liquid drops using smoothed particles.

Finally, we use the smoothed-particle method to study the highly-nonlinear gas-phase and dense-fluid-phase versions of *Rayleigh-Bénard instability*, the challenging numerical fluid dynamics problem of characterizing and distinguishing both the periodic and the chaotic convective flows of a compressible fluid, heated from below, in a gravitational field. In addition to the ideal-gas constitutive relations, we study also a dense-fluid model with nonideal thermal and mechanical equations of state. The model corresponds to a short-ranged repulsive interparticle pair potential.

The Rayleigh-Bénard problem has already been studied with conventional molecular dynamics [7–9] and, in the incompressible case, with grid-based continuum numerical methods. Goldhirsch, Pelz, and Orszag’s definitive continuum work [10] is readable, and contains a useful bibliography of numerical simulations. We discuss the chaotic irreversible behavior of the microscopic and macroscopic numerical techniques. Finally, we describe a hybrid scheme combining them.

The grid-free smoothed-particle technique, which we describe here, follows Monaghan’s ideas [3] very closely. It is well-suited to classroom introductions to chaos, to continuum mechanics, and to the numerical simulation of complex flows. We began our study of the method in a graduate Numerical Methods course, taught in the Department of Applied Science in the winter quarter of 1992–1993.

2. MOLECULAR DYNAMICS [1,2]

“Equilibrium Molecular Dynamics” simulates the time development of an isolated atomistic system of fixed composition, volume, and energy obeying classical mechanics. The goal is a solution of the first-order Hamiltonian or the second-order Newtonian equations of motion. For simplicity, we use Cartesian coordinates $\{r\}$ throughout. With the usual pairwise-additive potential energy $[\Phi(r) \equiv \sum \sum \phi_{i<j}]$ and point-mass kinetic energy $[K(p) \equiv \sum p^2/(2m)]$, combined in a separable Hamiltonian, $H \equiv \Phi(r) + K(p)$, the equations of motion can be written in two equivalent forms:

$$\left\{ \frac{dr}{dt} = \frac{p}{m}; \frac{dp}{dt} = F(r) \right\} \quad \text{or} \quad \left\{ \frac{d^2r}{dt^2} = \frac{F(r)}{m} \right\}.$$

The simplest method for solving the motion equations is Stoermer’s leapfrog scheme [1,11–14] which replaces the second-order Newtonian equations with a centered-difference approximation:

$$\frac{[r_{t+dt} - 2r_t + r_{t-dt}]}{(dt)^2} \equiv \frac{F(r_t)}{m}.$$

The “time step” dt is typically a few percent of a characteristic high-frequency vibrational period. The predominant errors in the approximate leapfrog trajectories are *phase* (as opposed to *amplitude*) errors. The phase errors are of order dt^2 , following from local integration errors of order dt^4 . At the expense of additional storage space, more-nearly-accurate solutions can be readily obtained using higher-order methods. The classic fourth-order Runge-Kutta method, with local errors of order dt^5 , is the most familiar of these. Another explicit fourth-order method [13; see footnote¹] which shares the time-reversible nature of Stoermer’s scheme, and, like it, requires only one force evaluation per step, provides new coordinates from the accelerations at *three* consecutive times:

$$\frac{[r_{t+2dt} - r_{t+dt} - r_{t-dt} + r_{t-2dt}]}{3(dt)^2} \equiv \frac{[5F_{t+dt} + 2F_t + 5F_{t-dt}]}{12m}.$$

The “results” generated by such a finite-difference scheme are the time evolutions of all the dynamical fluctuating quantities—that is, all those functions of the coordinates and momenta which are not constants of the motion. Familiar examples are the two- and three-body distribution functions, the stress tensor, the heat flux vector, and the kinetic temperature. Generally the values of the “continuum variables,” such as stress and temperature, are associated with individual atomic positions. The basis for interpreting the long-time-averaged results of equilibrium simulations, once transients have decayed, is Gibbs’ equilibrium statistical mechanics.

That theory, which assumes the equivalence of time averages and phase-space averages, establishes that equilibrium thermodynamic properties (the free energies and the thermal and mechanical equations of state derived from them) become independent of the choice of state variables for sufficiently-large isolated systems. For such large systems, both surface effects and fluctuations become negligibly small. The resulting large-system limit is referred to as the “thermodynamic limit.” In this limiting case, $N \rightarrow \infty$, the local fluctuations in the intensive variables associated with molecular dynamics become negligibly small, with amplitudes varying as $N^{-1/2}$. The validity of these ideas has been established by intercomparisons of simulation techniques: isoenergetic versus isothermal, and isobaric versus isochoric.

Away from equilibrium, in the most general case, both the time- and the space-dependences of concentrations, velocity, and energy need to be considered. Even when these are all absent, in homogeneous steady nonequilibrium states, additional nonequilibrium variables, such as fluxes or gradients of concentration, momentum, and energy, must be specified. At first glance, it appears that a nonequilibrium analog of the equilibrium “thermodynamic limit” cannot be achieved.

¹Like Stoermer’s, the fourth-order method has been rediscovered, too. See [1,14].

With fixed nonzero velocity and/or temperature gradients, larger and larger systems lead first to turbulence, and then to divergence. This conceptual problem can be avoided by using control forces to generate spatially homogeneous, near-equilibrium, steady states.

Sufficiently close to equilibrium, the nonlinear nonequilibrium effects, such as viscous heating, can be ignored. Accordingly, in parallel to the equilibrium thermodynamic limit, a large-system time-independent “hydrodynamic limit,” *can* be defined for homogeneous steady-state nonequilibrium systems [15], and approximated numerically in simulations, by using special control forces to maintain small deviations from equilibrium and to extract the resultant heat. Like Newton’s forces, the control forces are deterministic and time-reversible. By applying these not just at boundaries, but homogeneously, throughout the system, boundary-driven turbulence can be avoided.

The contribution of edge effects can also be avoided by using *periodic* boundary conditions. Then, for a one-component homogeneous spatially-periodic steady state in the resulting *hydrodynamic* limit, the equilibrium variables, density, velocity, and energy, need to be augmented by one or more nonzero components of the velocity gradient tensor, ∇v . The additional control forces required to maintain a steady state are applied homogeneously, throughout the system.

More realistic nonequilibrium systems have boundaries and are inhomogeneous. Simulating the corresponding nonequilibrium problems with molecular dynamics requires boundary forces capable of exchanging mechanical and thermal energy with the surroundings. The most general form of “Nonequilibrium Molecular Dynamics,” incorporates mechanical work, based on coordinate variations $\{\delta r\}$, as well as heat transfer, based on momentum variations $\{\delta p\}$. Many methods have been developed to implement this combination of thermodynamics with mechanics. The simplest of these extensions include either “Gaussian” or “Nosé-Hoover” thermostats to govern heat transfer [1,2]. These two approaches, unlike older alternatives based on the stochastic Langevin equation, retain the deterministic time-reversible nature of Newton’s equations, and can be solved by straightforward generalizations of Stoermer’s leapfrog scheme [1,16].

3. SMOOTHED-PARTICLE APPLIED MECHANICS [3,5]

The smoothed-particle technique for solving problems in applied mechanics was developed nearly 20 years ago and has since been applied to a number of difficult problems involving large deformations [4]. Applications have included the development of fluid instabilities, the formation of astrophysical structures, and the high-speed fracture and penetration of solids. In every case, the underlying equations to be solved are the same—the partial differential field equations of continuum mechanics—conservation of mass, momentum, and energy:

$$\begin{aligned}\frac{d\rho}{dt} &\equiv \frac{\partial\rho}{\partial t} + v \cdot \nabla\rho = -\rho\nabla \cdot v, \\ \frac{\rho dv}{dt} &\equiv \frac{\rho\partial v}{\partial t} + \rho v \cdot \nabla v = -\nabla \cdot P, \\ \frac{\rho de}{dt} &\equiv \frac{\rho\partial e}{\partial t} + \rho v \cdot \nabla e = -P : \nabla v - \nabla \cdot \mathbf{Q}.\end{aligned}$$

These equations, with initial and boundary conditions, form a closed system once the constitutive dependence (on the field variables $\{\rho, v, e, \nabla v, \nabla T\}$) of the pressure tensor P and the heat flux vector \mathbf{Q} is specified. Gravitational and electromagnetic fields can also be included. Because the continuous spatial variation of all the field variables, for the equations just given, is logically equivalent to an *infinite* number of discrete degrees of freedom, approximate solutions of these equations are based on series truncation, point interpolation, or volume averaging.

The smoothed-particle approach is based on interpolation among a set of irregularly-arranged moving grid points, the set of “smoothed particles.” The mean motion of these particles fluctuates about the macroscopic hydrodynamic flow. The smoothed particles, with masses $\{m\}$, are imagined to have their masses distributed in space according to a spatial probability density $w(r)$

which has a finite range h . Thus, there is no need to solve the continuity equation for the mass distribution. The local density can more easily be computed by summing up the contributions of nearby particles.

The weighting function $w(r)$ bears more than a superficial resemblance to the pair potential function $\phi(r)$ familiar from molecular dynamics. We give the details of this correspondence in Section 5. For the special case $h = 1$, Lucy's original choice for a weighting function [5],

$$w_L(r < 1) \equiv c_L(1 + 3r)(1 - r)^3,$$

is probably the simplest. Three typical weighting functions are shown in Figure 1 and described in more detail in Section 6. The constant c is chosen so that the spatial integral of w is unity. Thus, Lucy's normalization constant c_L has the values $\{\frac{5}{4}, \frac{5}{\pi}, \frac{105}{16\pi}\}$ in one, two, and three space dimensions.

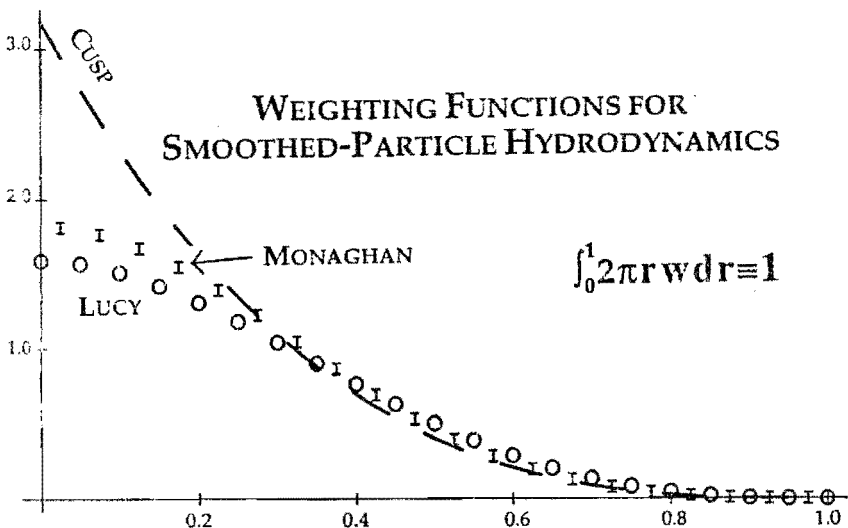


Figure 1. The three smoothed-particle weight functions described in the text are shown. In the analogy of smoothed-particle hydrodynamics with molecular dynamics, these correspond to soft repulsive potential functions.

In the simplest version of smoothed-particle applied mechanics, the density at each point is defined by summing the contributions from nearby particles:

$$\rho_j \equiv \sum m_i w(r_i - r_j),$$

where the self-density contribution ($i = j$) is included in the sum. Spatial averages $\langle f \rangle$ of other field quantities (such as the velocity) at a point r , according to this approach, are calculated in a similar way, by summing over the weight functions $\{w_j\}$ and field quantities $\{f_j\}$ associated with the nearby points $\{j\}$ lying within the range h of r :

$$\langle f \rangle \equiv \sum \frac{f_j m_j w(r - r_j)}{\rho_j}.$$

This formulation of averages is motivated by the advantage that the spatial gradients appearing in the continuum conservation equations can be expressed as simple sums over points involving the first derivative w' , of w .

$$\langle \nabla f \rangle \equiv \sum \nabla \left[\frac{f_j m_j w(r - r_j)}{\rho_j} \right] \equiv \sum \left[\frac{f_j m_j}{\rho_j} \right] \nabla w(r - r_j).$$

This expression for the smoothed-particle gradients exposes the underlying simplicity of the method. The resulting approximations to the partial differential equations for the time development of the field variables $\{\rho, v, e\}_j$ include a set of ordinary differential equations of motion for the time evolution of the smoothed-particle coordinates. These smoothed-particle ordinary differential equations closely resemble the ordinary differential equations of molecular dynamics. It needs to be emphasized that the distinction between v_i , the velocity of the i^{th} smoothed particle, and $\langle v \rangle_i$, the averaged hydrodynamic velocity at the location of the i^{th} particle (the latter includes the contributions from near neighbors) is conspicuously absent in most published accounts of this method. In molecular dynamics, this local difference in velocities is crucial. It defines the local kinetic temperature.

For a fluid or solid, made up of N particles, each with mass m , the smoothed-particle motion and energy equations take the form:

$$\begin{aligned} \frac{dv_i}{dt} &= -m \sum \left[\left(\frac{P_i}{\rho_i^2} \right) + \left(\frac{P_j}{\rho_j^2} \right) \right] \cdot \nabla_i w(r_{ij}); \\ \frac{de_i}{dt} &= \left(\frac{m}{2} \right) \sum \left[\left(\frac{P_i}{\rho_i^2} \right) + \left(\frac{P_j}{\rho_j^2} \right) \right] : v_{ij} \nabla_i w(r_{ij}) - m \sum \left[\left(\frac{Q_i}{\rho_i^2} \right) + \left(\frac{Q_j}{\rho_j^2} \right) \right] \cdot \nabla_i w(r_{ij}); \\ \rho_i &\equiv m \sum w(r_{ij}); \quad r_{ij} \equiv r_i - r_j; \quad v_{ij} \equiv v_i - v_j, \end{aligned}$$

where $P(\rho, e, \nabla v)$ is the pressure tensor, and $\mathbf{Q}(\rho, e, \nabla T)$ is the heat flux vector. These expressions can be derived by differentiating the smoothed-particle expressions for $\left(\frac{P}{\rho} \right)$ and $\left(\frac{Q}{\rho} \right)$. Because the momentum contributions to the members of each ij pair of particles sum to zero, the equation of motion conserves momentum exactly. Likewise, the motion and energy equations together provide a summed expression for the total energy, $E \equiv m \sum [(v^2/2) + e]_i$, which is *exactly* constant, furnishing a useful check on the numerical work.

The derivatives ∇v and ∇T can be obtained from somewhat different formulae based on differentiating the smoothed-particle expressions for $(v\rho)$ and $(T\rho)$:

$$\begin{aligned} \langle \nabla v \rangle &\equiv -m \sum \left[\frac{(v_i - v_j)}{\rho_{ij}} \right] \nabla_i w_{ij}; \\ \langle \nabla T \rangle &\equiv -m \sum \left[\frac{(T_i - T_j)}{\rho_{ij}} \right] \nabla_i w_{ij}, \end{aligned}$$

where the mean density ρ_{ij} can be chosen as the arithmetic or geometric mean of ρ_i and ρ_j . The symmetric formulation just given above is far from unique. Other approaches, which we used in our early work, can be found in Monaghan's review [3].

Though the ordinary differential equations just given bear a close resemblance to those of molecular dynamics, they are more complex in several ways. First, the *form of the weight function*, and its range, depend upon the judgment of the investigator. We will see, in Sections 6 and 7, that calculated results can be unreasonably sensitive to these arbitrary choices. Second, the accelerations depend upon an additional particle variable, the internal energy, as well as on the velocity gradient, plastic strain, and the like. The thermal equation of state, relating energy to temperature, and the mechanical equation of state, which gives the pressure, must be "self-consistent," satisfying a Maxwell relation $\frac{\partial^2 A}{\partial V \partial T} \equiv \frac{\partial^2 A}{\partial T \partial V}$, where $A(V, T)$ is the Helmholtz free energy. Third, rather than being consequences of interatomic forces, the *nonequilibrium* constitutive properties (bulk and shear viscosity, heat conductivity, yield strength, surface free energy, . . .) must be specified in advance.

Fourth, in integrating the smoothed-particle equations of motion, *three* separate sums over pairs (rather than just the one sum needed in molecular dynamics) must be carried out:

- (1) Calculation of the densities and temperatures.
- (2) Calculation of the velocity and temperature *spatial* gradients.
- (3) Calculation of the *time* derivatives $\frac{dv}{dt}$ and $\frac{de}{dT}$.

Each step requires the completion of its predecessors.

Fifth, the *forms of the hydrodynamic equations* underlying the approximation also depend on judgment, and allow corresponding choices among alternative sets of partial differential equations. For instance, the density could be calculated by integrating the continuity equation, $\frac{d(\rho v)}{dt} = -\nabla \cdot v$, rather than by summing the weight functions [3].

Finally, *many* finite-difference approximations to the differential equations are possible. For particular problems, some of these approximation methods are stable while others are not.

In the present work, we have considered a variety of weight functions, and discarded others, some of which produce unstable dynamics. We have not explored much variation in the basic continuum equations, but we have consistently avoided low-order integration errors and instabilities by using fourth-order Runge-Kutta integration. Once a particular problem is specified and a stable numerical approach has been validated and adopted, the highly-accurate fourth-order Runge-Kutta integrator could be replaced by a lower-order substitute.

4. SMOOTHED-PARTICLE APPLIED MECHANICS VS. EMBEDDED ATOMS

From the mathematical standpoint, the smoothed-particle approach to continuum mechanics resembles the completely-atomistic “embedded-atom” view [17] of metals. The embedded-atom approach has provided an extremely useful and flexible description of the many-body (that is, not just pairwise) interactions which give metals their unique structural, flow, and surface properties. Though the embedded-atom forces are a generalization of the usual pair-force models, their implementation is not particularly costly. Relative to molecular dynamics, the densities in the embedded-atom model require an additional sum over all interacting pairs of atoms.

The embedded-atom approach views each atom as *embedded* in an electronic density distribution $\rho_e(r)$ composed of contributions from the atom’s near neighbors. Thus, the smoothed-particle weighting function $w(r)$ is analogous to the electronic distribution carried by a moving metal atom. In both cases, the ordinary differential equations of motion are functionals of the particle coordinates:

$$\frac{d^2 r}{dt^2} = \frac{F[\rho(\{r\})]}{m}.$$

The smoothed-particle approach is the more general because the smoothed-particle forces $\{F\}$, and energy changes $\{\frac{de}{dt}\}$, need not depend upon the densities $\{\rho(r)\}$ and energies $\{e(r)\}$ only. Additional time dependencies from the velocities (through the viscous contributions), the temperatures (through their heat-conduction contributions), and the past history (through the plastic strain) are also possible.

5. MOLECULAR DYNAMIC ANALOG OF SMOOTHED-PARTICLE MECHANICS

If we consider a two-dimensional ideal gas composed of particles with mass m , then the macroscopic mechanical and thermal constitutive equations of state are $\{P = \rho e; e = kT/m\}$, where P is the hydrostatic pressure, T is the temperature, and k is Boltzmann’s constant. For an isentropic flow,

$$\dot{e} \equiv T \dot{s} + \left(\frac{P}{\rho^2}\right) \dot{\rho} = 0 + \left(\frac{P}{\rho^2}\right) \dot{\rho}.$$

From the ideal-gas constitutive relations, the time-rate-of-change of the internal energy e provides

a relation linking the time derivatives of the density and pressure:

$$\dot{e} \equiv \left(\frac{d}{dt} \right) \left(\frac{P}{\rho} \right) = - \left(\frac{P}{\rho^2} \right) \dot{\rho} + \left(\frac{\dot{P}}{\rho} \right).$$

From the equality of these two relations for \dot{e} , it follows that $\frac{dP}{d\rho} = \frac{2P}{\rho}$, so that P is proportional to ρ^2 for such an isentropic process. If, for convenience, we were to choose the proportionality constant equal to $\frac{1}{2m^2}$, the smoothed-particle ideal-gas motion equations would become

$$\frac{m dv_i}{dt} = - \sum \nabla_i w(r_{ij}); \quad \frac{m de_i}{dt} = \left(\frac{1}{2} \right) \sum v_{ij} \cdot \nabla_i w(r_{ij}),$$

where, as before, v_{ij} is the relative velocity, $v_i - v_j$. These smoothed-particle equations are *identical in form* to those describing the conservative molecular dynamics of a system of point particles interacting with pair potential $\phi(r) \equiv w(r)$:

$$\frac{m dv_i}{dt} = - \sum \nabla_i \phi_{ij}; \quad \frac{m de_i}{dt} = \left(\frac{1}{2} \right) \sum v_{ij} \cdot \nabla_i \phi_{ij},$$

where the internal energy e_i *does not* include Particle i 's kinetic energy $(mv_i^2)/2$. If both the kinetic and the potential energy contributions were included, then the time derivative would depend on the mean velocity, rather than the relative velocity, of each pair:

$$\left(\frac{d}{dt} \right) \frac{mv_i^2 + \sum \phi_{ij}}{2} \equiv \left(\frac{1}{2} \right) \sum (v_i + v_j) \cdot \nabla_i \phi_{ij}.$$

Thus, for the special isentropic ideal-gas case, $P \propto \rho^2$, the continuum weighting function w corresponds exactly to an atomistic pair potential energy ϕ : **the time evolution of an isentropic smoothed-particle ideal fluid, with weighting function $w(r)$, is identical to that of the time evolution of a nonideal system of N particles interacting with pair potential $\phi(r) \equiv w(r)$.**

Though exact, this result *appears* to be paradoxical, because the smoothed-particle description is spatially very highly correlated. From the atomistic viewpoint the smoothed-particle description resembles a *very* dense fluid. Each particle interacts with dozens of others. In a dense molecular dynamical system, viscous effects, both shear and bulk, as well as thermal conductivity, would typically lead to dissipation on a time scale of picoseconds. These well-established and well-understood dissipative effects can be readily analyzed through computer simulation [18] and have a rigorous theoretical link to equilibrium autocorrelation functions through Green and Kubo's linear-response theory [19].

Thus, it appears to be paradoxical that the (smoothed-particle) description of an *ideal* fluid includes within it a dense-fluid dynamics which seems likely to show dissipation. In fact, the corresponding molecular dynamical system might well also exhibit a *solid* phase or phases, with a well-defined plastic yield strength, further confounding the interpretation of the *solid*-phase molecular dynamics as representing the smoothed-particle mechanics of an ideal *fluid*.

These paradoxes can be resolved, in part, by noting that, as the number density of smoothed particles is increased, the corresponding dissipative coefficients approach zero, vanishing in the high-density limit. In this (unobtainable) limit the smoothed-particle approach is exact. For instance, it is a simple calculation to show that, in one dimension, the (solid-phase) vibrational frequencies are proportional to $\frac{1}{N}$ if the range of the weighting function, h , is held fixed. The spatial average of the vibrational force constant $\nabla^2 \phi(r)$ is likewise zero, in one, two, or three dimensions because the force, $-\nabla \phi$, vanishes at $r = h$.

Of course, these limiting cases are purely hypothetical mathematics, and not physics. An interesting purely-mathematical problem is the characterization of the opposite *low*-density limit,

in which the smoothed particles occasionally collide, as in kinetic theory. This limit has not been discussed, but might well be an interesting research area.

As smoothed-particle applied mechanics approaches continuum mechanics, we expect that any dissipation found for an ideal gas would disappear. On the other hand, a molecular dynamical simulation would certainly reveal a conversion of macroscopic long-wavelength velocity gradients to heat. Such dissipation lies outside the Euler equations of inviscid hydrodynamics. These considerations raise an interesting question: do the inviscid nonconducting smoothed-particle equations exhibit irreversibility?

From the formal standpoint, the isentropic smoothed-particle equations have the same time-reversibility characteristics as do Newton's atomistic equations of motion: replacing t by $-t$, v by $-v$, and $\frac{d}{dt}$ by $-\frac{d}{dt}$ leaves the equations of motion unchanged. On the other hand, the smoothed-particle phase space $\{r, v, e\}$ contains the energy densities in addition to the coordinates and momenta of molecular dynamics. For this reason, even the time evolution of the isentropic smoothed-particle equations does not satisfy Liouville's Theorem for the phase-space probability density f . For molecular dynamics, where the density depends on $\{r, p\}$ as well as the time, the theorem follows from Hamilton's equations of motion:

$$\left(\frac{df}{dt}\right)_{MD} = \frac{\partial f}{\partial t} + \left(\frac{dr}{dt}\right) \left(\frac{\partial f}{\partial r}\right) + \left(\frac{dp}{dt}\right) \left(\frac{\partial f}{\partial p}\right) \equiv -f \left[\left(\frac{\partial \dot{r}}{\partial r}\right) + \left(\frac{\partial \dot{p}}{\partial p}\right) \right] \equiv 0,$$

where we have in mind, but do not explicitly indicate, *sums* of the derivatives, over all degrees of freedom. Thus, the co-moving time derivative $\left(\frac{df}{dt}\right)_{MD}$ of the atomistic phase-space probability density $f(r, p, t)$ vanishes.

For smoothed-particle applied mechanics, the additional dependence, on energy, changes the flow equation:

$$\begin{aligned} \left(\frac{df}{dt}\right)_{SPAM} &= \frac{\partial f}{\partial t} + \left(\frac{dr}{dt}\right) \left(\frac{\partial f}{\partial r}\right) + \left(\frac{dp}{dt}\right) \left(\frac{\partial f}{\partial p}\right) + \left(\frac{de}{dt}\right) \left(\frac{\partial f}{\partial e}\right) \\ &\equiv -f \left[\left(\frac{\partial \dot{r}}{\partial r}\right) + \left(\frac{\partial \dot{p}}{\partial p}\right) + \left(\frac{\partial \dot{e}}{\partial e}\right) \right] \equiv -f \left(\frac{\partial \dot{e}}{\partial e}\right) \neq 0. \end{aligned}$$

Again, this abbreviated flow equation represents a sum over all particle coordinates, momenta, and energies. In the smoothed-particle case, the last term is not necessarily zero. The smoothed-particle phase-space probability density can change with time.

To investigate the possibility of an intrinsic dissipation in smoothed-particle applied mechanics (which has some unpublished support at the level of folklore), we investigated the simple 36-mass doubly-periodic two-dimensional system shown in Figure 2, using two different values for the range of $w, h = 1.5$ (so that a typical smoothed particle interacts with six neighbors) and $h = 2.5$ (so that a typical particle interacts with 18 neighbors). We began the simulations with a perfect 6×6 square-lattice arrangement of the ideal-gas particles, with sets of randomly oriented velocities, chosen such that the overall momentum vanishes and with unit kinetic energy initially, equally divided between the x and the y velocity components. As usual, we avoided all low-order truncation errors associated with time differencing the motion equations by using a locally-fourth-order-accurate Runge-Kutta integration scheme with a relatively-small time step.

In a typical case, with a Runge-Kutta time step of 0.05 and with the range of the weight function, $h = 1.5$, the internal energy showed fluctuations, of order 3%, $\approx \frac{1}{N}$, but with no tendency to increase or decrease over a run of 10,000 steps. The total energy defined by summing the individual particle values of $(mv^2)/2$ and me , was, as expected, constant.

Fluctuations are inherent in the smoothed-particle method and these persist in the limit $dt \rightarrow 0$. Cutting the time step in half produces a slightly different approximate trajectory, but likewise with no long-term energy drift. The initially-small $[10^{-12}]$ offset separating two neighboring trajectories (both of which presumably exhibit Lyapunov instability, with the offset growing

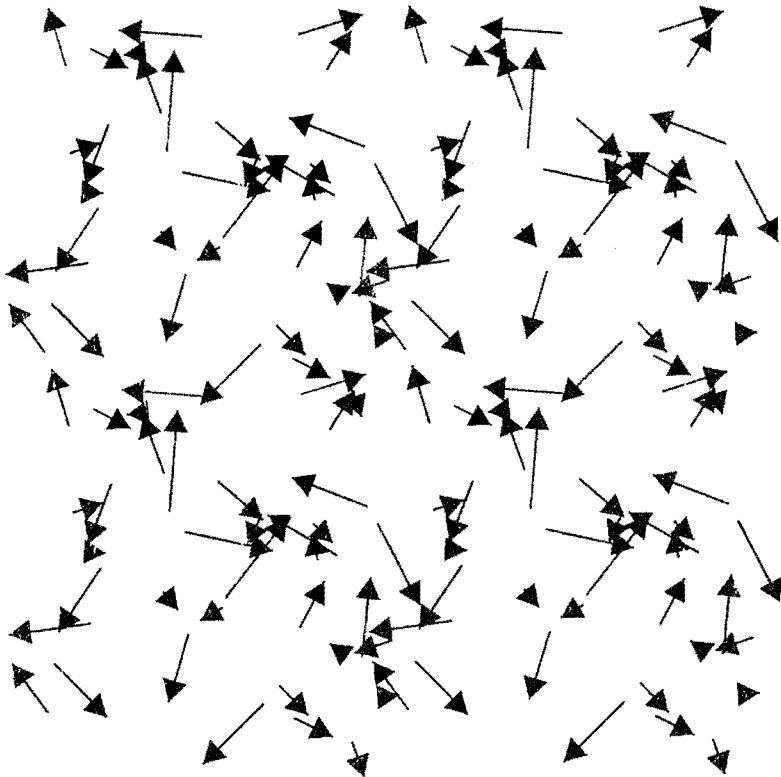


Figure 2. Isolated 36-mass periodic system using Lucy's weight function with $h = 2.5$. With the ideal-gas constitutive relation $P \equiv \rho e$ the motion of these particles conserves energy exactly.

as $e^{\lambda t}$) becomes macroscopic [10⁰] after several hundred time steps. We conclude that an accurate solution of the smoothed-particle ideal-gas equations of motion is typically chaotic, and contains no intrinsic dissipation mechanism, despite the exact analogy with chaotic nonlinear molecular dynamics.

6. VALIDATION OF THE SMOOTHED-PARTICLE APPROACH

6.1. Structural Validation of the Smoothed-Particle Approach

For the smoothed-particle approach to give a faithful representation of fluid flow, it is desirable that no regular arrangement of the particles lead to a structure resisting limiting zero-frequency shear. In any "fluid" structure, it should be possible for the nodes to move, relative to each other, without inducing any permanent shear stress. The magnitude of such an undesirable and spurious stress could be estimated by using the analogy with molecular dynamics.

From the motion equations discussed in Section 5, it is clear that the smoothed-particle equations, for a homogeneous constant-pressure, constant-density fluid, are *isomorphic* to the equations of molecular dynamics (because $\frac{P}{\rho^2}$ would be the same for all particles). Thus, the smoothed-particle trajectories, for a given weighting function $w(r)$ are identical to molecular-dynamics particle trajectories with w playing the role of a potential function. Thus, the *shear* stability of any combination of weighting function and nodal structure can be evaluated for smoothed particles by computing the analog of the solid-phase elastic constants (ratios of stress to strain) for atoms.

A numerical stability check is easy to make. Simply compute the analog of the energy change, induced by a small shear strain, $\Delta \sum \phi_{ij} \approx \Delta \sum w_{ij}$. A more-complete (Fourier) analysis would evaluate the analog of the entire solid-phase quasiharmonic vibrational spectrum in order to ensure that no shear deformation of a smoothed-particle fluid meets with a sizable elastic response.

In the two-dimensional case, the most likely stable symmetric structures are the square lattice (with four nearest neighbors) and the triangular lattice (with six). We explored the stability of both these structures using three weight functions. In each case, these functions vanish beyond $r = 1$, and are normalized, so that $2\pi \int_0^1 r w(r) dr \equiv 1$. The three forms we chose for w , $\{w_L, w_C, w_M\}$, are, respectively, Lucy's original choice, a simpler one, with a cusp at the origin, and the two-part spline recommended by Monaghan:

$$w_L = \left(\frac{5}{\pi}\right) (1 + 3r)(1 - r)^3 \quad \text{and} \quad w_C = \left(\frac{10}{\pi}\right) (1 - r)^3, \quad \text{both for } 0 < r < 1;$$

$$w_M = \left(\frac{40}{7\pi}\right) (1 - 6r^2 + 6r^3), \quad \text{for } r < 0.5, \quad \text{and} \quad \left(\frac{80}{7\pi}\right) (1 - r)^3, \quad \text{for } 0.5 < r < 1.$$

We found that Lucy's and Monaghan's weight functions, w_L and w_M , provided smoother more-nearly-accurate representations of the density. Usually, depending upon the range of the weight function (or, equivalently, on the density of points), one or the other of the two periodic lattices was stable. Occasionally both were stable, or neither was stable. We explored lattice stability by computing the energy change associated with a small shear of the lattice, $\varepsilon_{xy} = 0.01$. These calculations provided no decisive evidence for the shear stability of one weight function over the other. On the other hand, the cusp weighting function provides relatively poor estimates of the overall density, with errors of the order of a few percent. We conclude that the smoothed-particle method does, in some cases, predict an ordered structure for a "fluid," but that the shear strength of such a fluid is negligibly small.

6.2. Linear Transport Validation of the Smoothed-Particle Approach

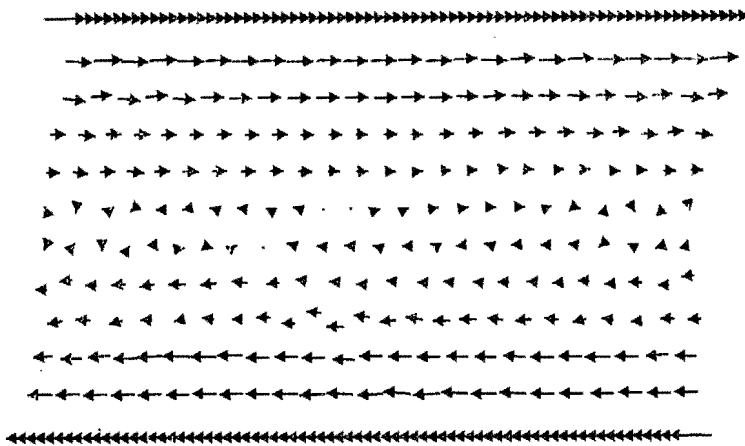


Figure 3. Typical configuration of a 384-particle ideal-gas system, with 72 steadily-moving particles at the top and at the bottom. There are 240 bulk smoothed particles. The vertical boundaries are periodic. In this simulation, the top boundary moves to the right (with speed 0.5) while the bottom boundary moves to the left (with the opposite velocity). Both the shear viscosity and the thermal conductivity are constants.

To test the adequacy of the smoothed-particle *energy transport*, we simulated a system of the type shown in Figure 3, but with fixed boundaries. It has two triple-density horizontal boundaries of 72 motionless particles, each with its internal energy (proportional to temperature) fixed. By acting as a high-density high-pressure barrier, these fixed boundary particles repel the bulk fluid and act as a rigid isothermal heat-conducting boundary. For convenience, we considered a system, periodic in the horizontal direction, and with a total of 144 boundary +240 bulk = 384 total particles. We used Lucy's weighting function with a range of 2.0. The width of the system was

24 and the top-to-bottom spacing between the horizontal rows of fixed boundary particles was 15, so that the mean bulk density was of order unity, as were the internal energy per particle and the temperature.

The thermal and mechanical equations of state of the gas were the ideal gas laws $\{P = \rho e; e = kT/m\}$. The heat capacity per unit mass, the shear viscosity coefficient, and the heat conductivity were all chosen equal to unity, independent of density and internal energy. After a decay of the initial transients, the flows of heat, into the system and out of the system, with boundary temperatures of 1.05 and 0.95, fairly soon (after a time of a few hundred, as expected from the ratio of system width, squared, to the thermal diffusivity) reached values in the neighborhood of the value expected from Fourier's Law, $24 \times (0.1/15) = 0.16$. The observed stationary value was actually somewhat lower, 0.128, indicating a surface-effect number dependence of order $N^{-1/2}$. An analogous calculation, using the cusp weighting function, also with a range $dr = 2$, provided a much worse steady-state heat flux estimate, 0.06. Considerable work needs to be done to systematize, understand, and reduce transport errors, separating weight-function effects from bulk and boundary contributions, for both fluids and solids, and in two dimensions as well as three.

To test smoothed-particle *momentum transport*, through the mechanism of shear viscosity, we used this same 384-particle geometry (See Figure 3) and set the temperatures of both horizontal boundaries equal to unity. The (horizontal) velocity component of the boundary particles was set equal to ± 0.5 , giving an overall shear strain rate, $\frac{du_x}{dy}$, equal to $\frac{1}{15}$. Under these conditions, the equations of motion include contributions from the two independent shear strain rates, $\dot{\epsilon}_{xx} - \dot{\epsilon}_{yy}$ and $\dot{\epsilon}_{xy}$. In our smoothed-particle representation, the underlying equations for the strain-rates at Particle i are:

$$\begin{aligned}\dot{\epsilon}_{xx} &= - \sum m w'_{ij} \frac{x_{ij} \dot{x}_{ij}}{r_{ij} \rho_{ij}}; \\ \dot{\epsilon}_{yy} &= - \sum m w'_{ij} \frac{y_{ij} \dot{y}_{ij}}{r_{ij} \rho_{ij}}; \\ \dot{\epsilon}_{xy} &= - \sum m w'_{ij} \frac{[x_{ij} \dot{y}_{ij} + y_{ij} \dot{x}_{ij}]}{r_{ij} \rho_{ij}},\end{aligned}$$

where ρ_{ij} is the symmetrized mean ij density, $(\rho_i \rho_j)^{1/2}$. As a measure of the arbitrariness in the smoothed-particle method, note that a symmetrized *arithmetic* mean, $(\rho_i + \rho_j)/2$, could, equally well, have been used. The sums, over j , include all interacting neighbors. The stresses have the usual form:

$$\begin{aligned}\sigma_{xx} &= -\rho e + \eta_V (\dot{\epsilon}_{xx} + \dot{\epsilon}_{yy}) + \eta (\dot{\epsilon}_{xx} - \dot{\epsilon}_{yy}); \\ \sigma_{yy} &= -\rho e + \eta_V (\dot{\epsilon}_{xx} + \dot{\epsilon}_{yy}) - \eta (\dot{\epsilon}_{xx} - \dot{\epsilon}_{yy}); \\ \sigma_{xy} &= \eta \dot{\epsilon}_{xy}.\end{aligned}$$

Usually the bulk viscosity η_V is ignored, as is appropriate for a low-density monatomic gas. Here, we have chosen to include it because of its usefulness in stabilizing the motion against transients in the initial phases of numerical solutions.

The equations of motion and the energy equation for Particle i are:

$$\begin{aligned}\ddot{x} &= m \sum w' \left\{ x_{ij} \left[\left(\frac{\sigma_{xx}}{\rho^2} \right)_i + \left(\frac{\sigma_{xx}}{\rho^2} \right)_j \right] + y_{ij} \left[\left(\frac{\sigma_{xy}}{\rho^2} \right)_i + \left(\frac{\sigma_{xy}}{\rho^2} \right)_j \right] \right\}; \\ \ddot{y} &= m \sum w' \left\{ x_{ij} \left[\left(\frac{\sigma_{xy}}{\rho^2} \right)_i + \left(\frac{\sigma_{xy}}{\rho^2} \right)_j \right] + y_{ij} \left[\left(\frac{\sigma_{yy}}{\rho^2} \right)_i + \left(\frac{\sigma_{yy}}{\rho^2} \right)_j \right] \right\}; \\ \dot{e} &= \left(\frac{-1}{2} \right) m \sum w' \left\{ \left(\frac{x_{ij} \dot{x}_{ij}}{r_{ij}} \right) \left[\left(\frac{\sigma_{xx}}{\rho^2} \right)_i + \left(\frac{\sigma_{xx}}{\rho^2} \right)_j \right] + \left(\frac{y_{ij} \dot{y}_{ij}}{r_{ij}} \right) \left[\left(\frac{\sigma_{yy}}{\rho^2} \right)_i + \left(\frac{\sigma_{yy}}{\rho^2} \right)_j \right] \right\}\end{aligned}$$

$$+ \left[\left(\frac{x_{ij} \dot{y}_{ij}}{r_{ij}} \right) + \left(\frac{y_{ij} \dot{x}_{ij}}{r_{ij}} \right) \right] \left[\left(\frac{\sigma_{xy}}{\rho^2} \right)_i + \left(\frac{\sigma_{xy}}{\rho^2} \right)_j \right] \left\} - m \sum \left[\left(\frac{\mathbf{Q}_i}{\rho_i^2} \right) + \left(\frac{\mathbf{Q}_j}{\rho_j^2} \right) \right] \cdot \nabla_i w(r_{ij}),$$

where $\mathbf{Q} \equiv -\kappa \cdot \nabla T$ is the heat flux, and κ is the heat conductivity; ∇T is the temperature gradient, given earlier.

Using again the Lucy weighting function, with range 2.0, and the ideal-gas constitutive relations (with η_V equal to zero), a viscous-flow simulation of 16,000 fourth-order Runge-Kutta steps was carried out ($dt = 0.05$). The resulting steady-state fluid shear stress could be measured directly, in either of two ways, by averaging σ_{xy} over the bulk particles or by averaging the momentum transferred, per unit length and time, to the horizontal boundary particles. Both stress estimates were somewhat less than the expected Navier-Stokes value, $\frac{1}{15}$. The cusp weighting function produced much more slip, and a much lower stress. With the Lucy weighting function, the actual momentum transfers at the boundaries were ± 1.17 , rather than the Navier-Stokes values, ± 1.6 . The total heat extracted at the boundaries, $2 \times 0.58 = 1.17$, agreed exactly with the actual work done by the shear forces. A different range for the weighting function, 1.5 rather than 2.0, resulted in a slightly-higher momentum transfer, ± 1.28 , still well short of the true hydrodynamic value. During the transient approach to the steady state, the mean shear stress (averaged over the volume) showed much less fluctuation (3%) than did the two surface estimates (20%) based on heat and momentum transfer. This disparity, in the size of the fluctuations, reflects the fact that fewer degrees of freedom participate in the surface estimates, so that the fluctuations in these estimates are larger.

The relative success of these two investigations, though with systematic surface errors of order $N^{-1/2}$, convinced us that bulk representations of ordinary linear transport phenomena are sufficiently well-represented by smoothed-particle applied mechanics to justify the study of more complex problems. Whether or not the smoothed-particle method is effective for systems with free boundaries still needed to be determined. Our progress on that question is described in the next section.

7. REPRESENTING SURFACES WITH SMOOTHED PARTICLE APPLIED MECHANICS

In our tests of shear flow, heat flow, and convection there were no “free surfaces,” by which we mean system boundaries free of all external forces. Free surfaces are inherent to most physical problems, with the creation of new surfaces, as in cutting, polishing, and penetrating, being particularly challenging problems in continuum mechanics. Smoothed-particle applied mechanics, like continuum mechanics, generally, ordinarily provides no explicit consideration of surface effects. It is often stated that surfaces are hard to describe with this method. The difficulty became abundantly clear to us in a class project designed to model the chaotic formation of the drops described in Shaw’s classic chaos problem, the “dripping faucet.” With the usual smoothed-particle treatment the “drops” evaporated!

In order further to investigate the response of the smoothed-particle method to surfaces, but in a more systematic way, we studied the relaxation of a rectangular sample of viscous fluid, with a width-to-height ratio of 2, again using the set of weight functions $\{w_L, w_C, w_M\}$, together with the simplest possible constitutive model, an energy-independent pressure, $p = \rho^2 - 1$ coupled to a density-and-energy-independent shear viscosity η . In these simulations, the cusp-based w_C function was much less stable and well-behaved than the two smooth choices, Lucy’s w_L and Monaghan’s w_M .

In all the stable cases, the qualitative results of the calculations were similar, with the initially-rectangular square-lattice sample relaxing to a somewhat more regular, but never really circular, overall shape. With shear viscous damping the final (motionless) state was completely stress-free, with each smoothed particle at unit density. Typical stable configurations are shown in Figure 4. There is a strong tendency for the particles to form chains, with neighboring chains of particles

separated by about the range of the weighting function w . In attaining the bulk density, particles at the “drop” boundary tend to have their near neighbors in directions parallel to that boundary. Thus, the distribution of particles is far from uniform. These pictures reflect the obvious, that smoothed-particle applied mechanics does not properly include surface tension.

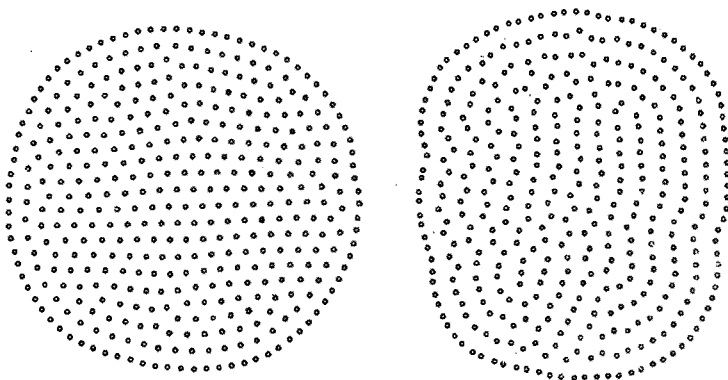


Figure 4. Relaxed 400-particle “drops” for the equation of state $P = \rho^2 - 1$ with a constant shear viscosity but *without* surface tension. The original shapes were rectangular.

How *could* surface energy be included in smoothed particle applied mechanics? In smoothed-particle simulations of radiation transport, Leigh Brookshaw finds surface particles by considering, for each particle, the weighted displacement sum over its neighbors:

$$\delta_i \equiv \sum w_{ij} r_{ij}.$$

In the bulk, such microscopic displacement vectors $\{\delta_i\}$ will exhibit small fluctuations around the overall direction of the macroscopic density gradient $\nabla\rho$. But at a boundary, the $\{\delta_i\}$ are vectors pointing away from the individual particles $\{i\}$ toward the outside.

This suggests several relatively convenient and realistic approaches to surface tension. The vector δ_i can itself be taken as proportional to the surface force on Particle i . This is the simplest approach, but requires an *ad hoc* scaling of the proportionality constant in order to reproduce the reduction of excess pressure (inversely proportional to the drop radius) with increasing drop size. Alternatively, the scalar sum $\sum \delta_i^2$ could be used as a measure of the surface free energy, with the vector δ_i defining the direction in which the maximum tensile surface stress acts. This gives, automatically, the correct dependence of surface tension on drop size. Figure 5 shows the resulting two-dimensional drops using the first of these ideas. The vectors $\{\delta_i\}$ were calculated with a weight function having twice the range of the bulk one. The results of these simulations, with surface tension stabilizing nearly circular drops, show that the cusp weight function w_C is clearly superior to w_L and w_M , in that more particles lie in the interior of the drop, so as to describe its structure. The cusp weight function greatly reduces the incidence of near neighbors.

With the ability of a few hundred smoothed-particles to treat, at least semiquantitatively, both transport processes and a variety of boundary conditions, we considered next a strongly nonlinear convective problem, the Rayleigh-Bénard instability of which Lorenz’ chaotic “butterfly attractor” is a caricature.

8. RAYLEIGH-BENARD INSTABILITY

The mechanical instability of a nearly-incompressible liquid, heated from below in a gravitational field, has been described—crudely—by Lorenz’ classic set of three coupled nonlinear equations [20], measured in a host of laboratory experiments, and simulated with molecular dynamics, using tens of thousands of particles [7–9]. The history of hydrodynamic investigations

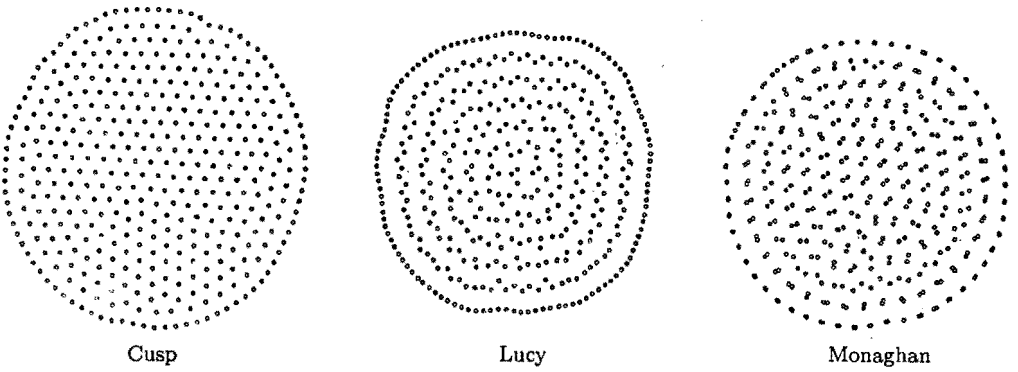


Figure 5. Relaxed 400-particle drops for the equation of state $P = \rho^2 - 1$ with a constant shear viscosity and *with* surface tension. The ranges of the weighting functions were all 2.5. The original shapes were rectangular. From left to right, the three weight functions are w_C , w_L , and w_M .

spans a century. The references listed in the work by Goldhirsch, Pelz, and Orszag [10] provide access to the early research.

We investigated first the gas-phase analog of this system, using the smoothed-particle method, and still retaining the two-dimensional ideal gas hydrostatic pressure-density-energy relation, with Lucy's weighting function. The problem requires also a gravitational field g . To maintain thermal contact at the upper [cold] boundary, g cannot be too large. We chose it in such a way that the maximum-to-minimum density ratio was not too large, always less than 2. We again incorporated shear viscosity [η] in this problem, and heat conductivity [κ] contributions to \dot{e} for each particle, as outlined by Monaghan [3].

Just as in our simpler transport test problems, the top and bottom boundaries were again made up of rows of particles at three times the normal linear density, as was shown in Figure 3. The boundary values of the coordinates, velocities, and energy densities were all held fixed.

The usual linear analysis of the Boussinesq approximation to the Rayleigh-Bénard problem deals with the linear instability of a nearly-incompressible fluid to convection rolls. For a "critical" value [of order $(2\pi)^4$] of the Rayleigh number R , convection rolls appear. R is given by

$$R = \left(\frac{\partial \ln \rho}{\partial T} \right)_P \left(\frac{\Delta T}{\Delta y} \right) \frac{g(\Delta y)^4}{\nu D},$$

where ν is the kinematic viscosity, D is the thermal diffusivity, and Δy is the height of the system. The convection rolls can give way to chaos (according to the simplified Lorenz model) at a Rayleigh number of order 20 times greater than that required for the rolls.

Convective chaos seems much harder to come by when the full equations are solved [10]. With a few hundred smoothed particles, our ideal-gas simulations required a much larger R , of order 10^6 , to generate unsteady flows. For an ideal gas [21] with a sizable temperature gradient, the Rayleigh number approaches the dimensionless ratio $(g(\Delta y)^3)/(\nu D)$. The importance of this ratio can be seen by comparing four different power levels characterizing the nonequilibrium flow, convection, conduction, buoyancy, and viscous dissipation. First, to see vigorous convection, it is necessary that the convective rate of energy transport exceed the (unstable) conductive rate:

$$\left(\frac{dE}{dt} \right)_{\text{CONVECTION}} = N kT \left(\frac{v}{\Delta y} \right) > \left(\frac{dE}{dt} \right)_{\text{CONDUCTION}} = \frac{\kappa T \Delta x}{\Delta y} \approx \kappa T,$$

giving a lower bound for the roll velocity:

$$v > \frac{\kappa \Delta y}{Nk}.$$

A second inequality results if we insist that the energy released by buoyancy must exceed the energy dissipation due to shear viscosity,

$$\left(\frac{dE}{dt}\right)_B = \rho \Delta x \Delta y g \Delta y \left(\frac{v}{\Delta y}\right) \approx \rho g \Delta y^2 v > \left(\frac{dE}{dt}\right)_V = \eta \Delta x \Delta y \left(\frac{v}{\Delta y}\right)^2 \approx \eta v^2 : \\ v < \frac{g \Delta y^2}{\nu}.$$

Thus, the dimensionless ratio of this upper velocity bound to the lower velocity bound, $g(\Delta y)^3/\nu D$, resembles the Rayleigh number.

Although the uncertain connection between the truncated incompressible linear theory and the highly-nonlinear simulation makes a definite prediction for the onset of rolls difficult, we had no difficulty generating rolls. The rolls can be portrayed in two distinct ways, first as *unsmoothed* $\{v\}$ and then as *smoothed* $\{\langle v \rangle\}$ velocity fields. The spatially-smoothed rolls have the more plausible appearance. The contrast of this 240-bulk-particle simulation with previous simulations, both

- (i) conventional continuum solutions which provide “fully resolved” fields [10] with a few thousand degrees of freedom and
- (ii) conventional molecular dynamics, with which the time-and-space averaged dynamics of as many as 57,600 atoms has been used,

suggests that the smoothed-particle approach to nonequilibrium simulations is well worth pursuing.

Accordingly, we have also studied the Rayleigh-Bénard problem using a macroscopic dense-fluid equation of state which corresponds to a simple interatomic pair potential [22] with three vanishing derivatives at the cutoff distance, $r = \sigma$:

$$\phi(r) = 100\epsilon \left[1 - \left(\frac{r}{\sigma}\right)^2\right]^4.$$

The *maximum* interaction strength is chosen equal to 100ϵ . This choice results in an effective collision diameter, at a temperature equal to $\frac{\epsilon}{k}$, of 0.8269σ . The mechanical and thermal equations of state in the vicinity of unit density, $N\sigma^2 = V$, and temperature, $kT = \epsilon$ were measured with molecular dynamics simulations. We represent the results of these simulations with simple quadratic forms. At unit (number) density and reduced temperature ρ , kT/ϵ , $PV/N\epsilon$ and $E/N\epsilon$ are, respectively, 1.00, 1.00, 5.04 and 1.44. For small deviations from this standard state, the following expansions apply:

$$\frac{PV}{N\epsilon} = 5 + 8\delta\rho + 2.5\delta\epsilon + 9\delta\rho^2 + 2\delta\rho\delta\epsilon; \\ \frac{kT}{\epsilon} = 1 - \delta\rho + 0.7\delta\epsilon - 0.8\delta\rho^2 - 0.5\delta\rho\delta\epsilon; \\ \frac{e}{\epsilon} \equiv \frac{E}{N\epsilon} = 1.443 + 1.5\delta\rho + 1.5\delta\tau + 2.4\delta\rho^2 + 1.2\delta\rho\delta\tau; \\ \delta\rho \equiv \left(\frac{N\sigma^2}{V}\right) - 1.000; \quad \delta\epsilon \equiv \left(\frac{E}{N\epsilon}\right) - 1.443; \quad \delta\tau \equiv \left(\frac{kT}{\epsilon}\right) - 1.000; \quad m = 1.$$

The first two expansions provide local-equilibrium pressures, which contribute to the accelerations $\{\frac{dv}{dt}\}$, and local temperatures, which drive the heat flux. Both contribute to $\{\frac{de}{dt}\}$. The additional expansion of energy as a series in $\delta\rho$ and $\delta\tau$ is made necessary by our thermal boundary conditions. On the boundaries of the box containing the Rayleigh-Bénard fluid, where energy must be calculated from the observed density and a specified boundary temperature, the special thermal equation giving $\frac{E}{N} \equiv e(\delta\rho, \delta\tau)$ is required. For such boundaries, the cusp weight function is less prone to “escapes” than are the smoother choices of Lucy and Monaghan. Once start-up

transients have relaxed, escapees (which require reflection and replacement within the system) are rare using the cusp weight function. We found that a bulk viscosity coefficient equal to the shear viscosity was useful in stabilizing the initial phases of dense-fluid Rayleigh-Bénard simulations.

Figure 6 shows two typical resulting flow patterns, using the averaged-flow representation for $\langle(\rho v)_i\rangle \equiv m \sum w_{ij} v_j$, for this simple model of a dense fluid. The general impression that movies of these simulations provide is the presence of chaotic velocity fluctuations over a wide range of wavelengths. We can anticipate that a quantitative comparison of the particle simulation with more-traditional continuum methods would bear out this emphasis of fluctuations by smoothed-particle applied mechanics.

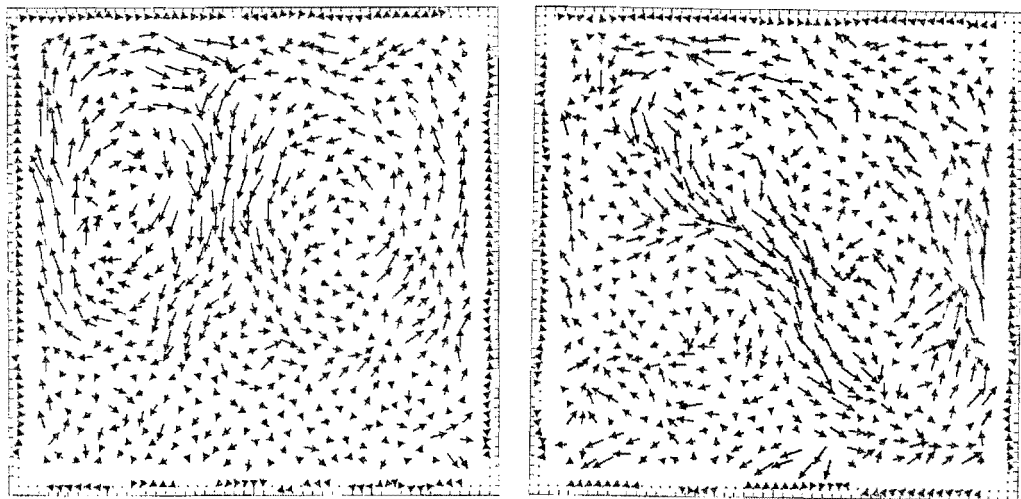


Figure 6. Two roll patterns $\{\langle v \rangle\}$ for a dense-fluid Rayleigh-Bénard flow with cold and hot boundary temperatures of 0.50 and 10.00. The mean bulk density and number density are both unity. The shear viscosity and thermal conductivity are both equal to 0.1 and the range of w_C is 2.5.

9. IRREVERSIBILITY AND CHAOS

In nonequilibrium statistical mechanics, the “molecular chaos,” described by Boltzmann, is ubiquitous. It is amusing to find that it also underlies the smoothed-particle continuum approach to hydrodynamics. In smoothed-particle applied mechanics, a truly stationary state, without fluctuations, is possible only if the underlying w -fluid freezes. This observation suggests a promising research area. The usual macroscopic hydrodynamic equations lose the microscopic chaos inherent in the fluids they describe by ignoring fluctuations. When fluctuations are important then smoothed-particle simulations provide a natural way to include them.

Chaotic fluctuations can be quantified by measuring the Lyapunov spectrum. The spectra describe the exponential growth and decay rates for perturbations to the solutions of the differential equations. The calculations are relatively expensive to carry out because the complete spectrum, for a system described by I time-dependent variables, requires the solution of $I + 1$ sets of I differential equations. Comparisons of approximate continuum studies of Lyapunov spectra with accurate molecular counterparts suggested that the two types of spectra have similar shapes [21]. We have explored the Lyapunov spectrum for a periodic two-dimensional ideal gas, using 16 smoothed particles. The complete spectra of 80 Lyapunov exponents (two coordinates, two velocities, and an internal energy for each particle) resulting from two such studies are shown in Figure 7. The spectrum has a shape reminiscent of that for a two-dimensional solid. It appears that the exponents associated with the energy vanish. There are eight pairs of these. Though we have not been able to prove that this should be the case, the numerical work suggests it. Two vanishing exponents are required by the time-symmetry of the equations of motion. Otherwise, the

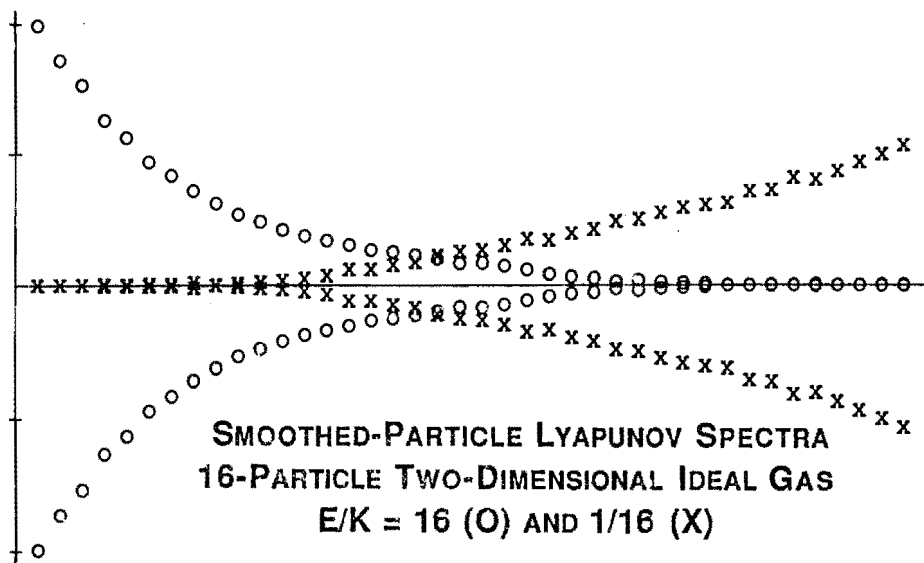


Figure 7. Lyapunov spectra for two-dimensional ideal gases made up of 16 smoothed particles, each with unit mass and described by Lucy's weighting function with a range of 1.5. The particles originally occupied a perfect triangular lattice, with a periodic area $4 \times (12)^{1/2}$. The initial ratios of internal to kinetic energy are indicated.

spectrum exhibits the expected Smale-pair symmetry, with 40 sets of paired exponents $\{\lambda, -\lambda\}$, and strongly resembles many-body spectra obtained from solid-phase atomistic studies [22].

Goldhirsch, Pelz, and Orszag emphasize the difficulty in establishing chaos, from numerical solutions, in systems of partial differential equations. There is no doubt that at sufficiently small Rayleigh numbers the Rayleigh-Bénard system does exhibit nonconvective solutions. In molecular dynamics, on the other hand, chaos is relatively easy to quantify, provided that the time integration is accurate. It occurs even in one- and two-body systems [23].

To approach the description of flows given by continuum mechanics, the limit of a large number of degrees of freedom must be taken. This limit can be approached in many different ways, by refining a regular spatial mesh or by introducing many smoothed particles. There is no logical reason to insist on a regular grid or to prefer one approach to the other. In any case, the limit is mathematical only, while the physical features of simulations are statistical in nature. Thus, our results suggest that the fluctuations in a simulation can depend very much on the choice of approximation method.

10. PARALLEL PROCESSING AND HYBRID SIMULATIONS

There is no difficulty in treating as many as 10,000 atoms or 10,000 smoothed particles in a single-processor simulation. Even such a modest calculation is prohibitively expensive unless the system is first subdivided into cells, of width equal to the range of $\phi(r)$ or $w(r)$, so that only interactions between neighboring cells need to be considered. When an additional, coarser cell subdivision is repeated on a larger scale, the larger cells can be associated with individual processors in a massively-parallel computer. In this way, millions of atoms or smoothed particles can be treated at present, with billions in the near term [6].

Even so, the twin requirements of atomistic detail (for realism) and micron size (for relevance) can only be met through hybrid models which combine the microscopic and macroscopic approaches. Of many possibilities, smoothed-particle applied mechanics is aesthetically appealing, as a hybrid base, because its structure resembles that of molecular dynamics. How can the two simulation methods best be combined?

The simplest possible prototypical hybrid scheme treats two-dimensional atoms and smoothed particles with identical masses, with comparable force- and weight-function ranges, and with a vanishing laboratory-frame velocity. Private densities and kinetic energies can then be calculated for all particles, both atoms and smoothed particles, in the same way, $\rho_i \equiv m \sum w(r_{ij})$; $kT_i \equiv (m^2/\rho_i) \sum w(r_{ij}) v_j^2$. The accelerations of the atoms and particles are calculated by superposing two kinds of contributions:

$$-\left(\frac{1}{m}\right) \nabla \phi \quad \text{or} \quad -m \left[\left(\frac{P_i}{\rho_i^2}\right) + \left(\frac{P_j}{\rho_j^2}\right) \right] \cdot \nabla_i w(r_{ij}),$$

where P_i is the pressure tensor for particle i . In order that these contributions sum to zero in a pairwise way, it is convenient to use the atomistic forces for any pairs involving at least one atom, and to use the continuum force for only those pairs involving two continuum particles.

This somewhat arbitrary allocation of force types conserves momentum, and is also exactly consistent with energy conservation provided that the energy contains both "potential" and "internal" contributions. Potential energies, obtained by summing pair potential contributions, $\phi(r)/2$, are allocated to all pair members, either atomistic and smoothed, which interact with an atom. Internal energies, for smoothed particles only, are computed by integrating the smoothed-particle equation for $\frac{de}{dt}$. The resulting total energy

$$E = \sum \frac{mv^2}{2} + \sum me + \sum \phi,$$

is a constant of the motion. Note that the second sum involves only smoothed particles, while the first and third can include contributions from all particles.

We have evaluated this scheme by using the same series of tests used to evaluate smoothed-particle approaches: first, equilibrium periodic simulations, next, linear transport simulations, and, finally, the nonlinear Rayleigh-Bénard problem. We have not yet carried out a detailed study of methods for (i), changing particle type during simulation and (ii), changing particle size as a function of time and location. The partial results obtained so far all suggest that this general approach is a viable method for large-scale simulations of flows combining atomistic and continuum parts. The main nonphysical feature of the present hybrid scheme is the gradual dissipation, through viscosity and heat conduction, of the atomistic kinetic energy, by the adjacent continuum.

11. CONCLUSIONS

Time and money requirements for modern structural and flow programs make intercomparisons within and between groups of investigators increasingly difficult. The widespread use of smoothed-particle applied mechanics will perhaps exacerbate this trend. The many choices underlying a calculation, both in characterizing the numerical approximations and in formulating constitutive equations, conspire against replication. Relatively simple equations of state, $P = \rho^2$ or $\rho^2 - 1$, for instance, round numbers of particles, 100 or 1000, and easily reproducible boundary conditions would all be helpful in countering the trend toward computational complexity. The temptation to avoid cross checking as problems become more complicated must be avoided. With this one caveat, smoothed-particle applied mechanics appears to be a very useful component of such validation programs.

Relatively rapid advances in hardware, coupled with much slower advances in software mandate that the simplest methods be used for simulation. These methods are also more easily implemented and checked, and the results are more easily communicated to others. They are ideal both for students and for research investigations. Nevertheless, smoothed-particle applied mechanics has many loose ends: the assumed constitutive properties $P(\rho, T)$, $e(\rho, T)$, $\eta(\rho, T)$, $\eta_V(\rho, T)$,

$\kappa(\rho, T)$; the prescribed boundary conditions, and the *ad hoc* weighting functions. Reproducibility, the *sine qua non* of science, can only be obtained with diligence. The use of an accurate time integrator (here the classic fourth-order Runge-Kutta method) avoids possible discrepancies and instabilities from lower-order difference schemes.

The close kinship which we have established here between molecular dynamics and smoothed particle dynamics has proved very helpful in developing a hybrid interface linking the two approaches.

REFERENCES

1. W.G. Hoover, *Computational Statistical Mechanics*, Elsevier, Amsterdam, (1991).
2. M.P. Allen and D.J. Tildesley, *Computer Simulation of Liquids*, Oxford University Press, (1987).
3. J.J. Monaghan, Smoothed particle hydrodynamics, *Annual Review of Astronomy and Astrophysics* **30**, 543 (1992).
4. H.E. Trease, M.J. Fritts, and W.P. Crowley, Editors, Advances in the free-Lagrange method, *Lecture Notes in Physics*, #395, Springer-Verlag, Berlin, (1991).
5. L.B. Lucy, A numerical approach to the testing of the fission hypothesis, *Astronomical Journal* **82**, 1013 (1977).
6. W.G. Hoover, A.J. De Groot, and C.G. Hoover, Massively parallel computer simulation of plane-strain elastic-plastic flow via nonequilibrium molecular dynamics and Lagrangian continuum mechanics, *Computers in Physics* **6**, 155 and cover (1992).
7. M. Mareschal, Microscopic simulations of instabilities, In *Microscopic Simulations of Complex Flows* (Edited by M. Mareschal) *NASI Series B: Physics*, Plenum, New York, (1990).
8. D.C. Rapaport, Molecular dynamics study of Rayleigh-Bénard convection, *Physical Review Letters* **60**, 2480 (1988).
9. D.C. Rapaport, Temporal periodicity in microscopic simulation of Rayleigh-Bénard convection, In *Microscopic Simulations of Complex Hydrodynamic Phenomena* (Edited M. Mareschal and B.L. Holian), *NASI Series B: Physics*, Plenum, New York, (1992).
10. I. Goldhirsch, R.B. Pelz, and S.A. Orszag, Numerical simulation of thermal convection in a two-dimensional finite box, *Journal of Fluid Mechanics* **199**, (1) (1989).
11. J.B. Gibson, A.N. Goland, M. Milgram, and G.H. Vineyard, Dynamics of radiation damage, *Physical Review* **120**, 1229 (1960).
12. L. Verlet, Computer experiments on classical fluids, *Physical Review* **159**, 98 (1967).
13. W.E. Milne, *Numerical Calculus*, Princeton University Press, (1949).
14. D. Levesque and L. Verlet, Molecular dynamics and time reversibility, *Journal of Statistical Physics* **72**, 519 (1993).
15. W.G. Hoover and H.A. Posch, Second-law irreversibility, and phase-space dimensionality loss, from time-reversible nonequilibrium steady-state Lyapunov spectra, *Physical Review E* **49**, 1913 (1994).
16. B.L. Holian, A.J. De Groot, W.G. Hoover, and C.G. Hoover, Time-reversible equilibrium and nonequilibrium isothermal-isobaric simulations with centered-difference Stoermer algorithms, *Physical Review A* **41**, 4552 (1990).
17. S.M. Foiles, M.I. Baskes, and M.S. Daw, Embedded-atom-method functions for the fcc metals Cu, Ag, Au, Ni, Pd, Pt, and their alloys, *Physical Review B* **33**, 7983 (1986).
18. W.G. Hoover, D.J. Evans, R.B. Hickman, A.J.C. Ladd, W.T. Ashurst, and B. Moran, Lennard-Jones triple-point bulk and shear viscosities. Green-Kubo theory, Hamiltonian mechanics, and nonequilibrium molecular dynamics, *Physical Review A* **22**, 1690 (1980).
19. D.A. McQuarrie, *Statistical Mechanics*, Harper and Row, New York, (1956).
20. E.H. Lorenz, Deterministic nonperiodic flow, *Journal of the Atmospheric Sciences* **20**, 130 (1963).
21. Wm.G. Hoover, C.G. Hoover, A.J. De Groot, and T.G. Pierce, Microscopic and macroscopic dynamics, In *Proceedings of the Second International Austrian Conference on Parallel Computing, Gmunden*, (October 4-6 1993).
22. H.A. Posch and W.G. Hoover, Equilibrium and nonequilibrium Lyapunov spectra for dense fluids and solids, *Physical Review A* **39**, 2175 (1989).
23. B. Moran, W.G. Hoover, and S. Bestiale, Diffusion in a periodic Lorentz gas, *Journal of Statistical Physics* **48**, 709 (1987).